RSC Advances

PAPER

View Article Online
View Journal | View Issue

Cite this: *RSC Adv.*, 2018, **8**, 35973

High binding ability ligand controlled formation of $CsPbX_3$ (X = Cl/Br, Br, I) perovskite nanocrystals with high quantum yields and enhanced stability†

Hongbo Xia,[a] Suli Wu,*[a] Lu Li[b] and Shufen Zhang[a]

Received 30th September 2018
Accepted 16th October 2018

DOI: 10.1039/c8ra08102f

rsc.li/rsc-advances

$CsPbX_3$ NCs with both high photoluminescence quantum yields (PLQYs) and enhanced stability have been obtained by using high binding ability ligands. As a result, the $CsPbI_3$ NCs prepared using palmitic acid and oleylamine as ligands have high PLQY (up to 92%), and the PLQYs of $CsPbX_3$ perovskite NCs can be sustained for one month with a slight decrease. Impressively, the presence of palmitic acid and stearic acid can dramatically improve the chemical stability of $CsPbX_3$ NCs. Importantly, ^{1}H NMR measurements indicate that much more palmitic acid remained on the surface of $CsPbX_3$ NCs than oleic acid after purification using solvent, suggesting the higher binding ability of palmitic acid than oleic acid. Finally, the fabricated perovskite NCs were used as luminescent inks and phosphors of white light emitting diodes.

Introduction

In recent years, perovskite semiconductors have received enormous attention due to their excellent photophysical properties such as small exciton binding energies, broadly tunable photoluminescence, high photoluminescence quantum yields (PLQYs) and narrow bandwidth. Up to now, perovskites have been applied in light-emitting devices (LEDs),[1] solar cells[2–4] and photodetectors.[5,6] In the past few years, both the hybrid and all-inorganic perovskites were reported to possess excellent optical properties.[7] In particular, the all-inorganic perovskites demonstrate higher stability resisting water, heat and continuous UV-light illumination than the hybrid ones.[8] Thus, the all-inorganic perovskites have gained the intensive attention of researchers.[9–12] As one of the inorganic perovskites, $CsPbX_3$ (X = Cl/Br, Br and I) perovskites have been prepared through hot-injection,[13] microwave-assisted,[14] room-temperature strategy,[15] and solvothermal methods.[8] To date, different kinds of $CsPbX_3$ perovskite such as nanocubes,[16] nanoplates,[17] nanowires[18] and nanorods,[19] have been synthesized by tuning the reaction parameters. Despite all these achievements and their relatively higher stability than hybrid perovskites, the stability of all-inorganic perovskites still needs to be improved further to satisfy their real applications.

Recently, lots of efforts have been devoted to improve the stability of the all-inorganic perovskites by silicone resin coating, polymer encapsulation and embedding perovskites into organic or inorganic matrix.[20–24] Usually, the reported modification methods need two steps: the preparation of $CsPbX_3$ perovskite NCs, and the modification of perovskite NCs by above mentioned inorganic or polymer matrix.[22,23,25–29] Although these approaches effectively increased the stability of perovskite NCs, the formation of perovskites/inorganic or organic composites usually obviously decrease the PLQYs and luminescence lifetimes of perovskites.[23,26,28,30] Hence, it is important to develop a strategy for enhancing their stability and maintaining high PLQY simultaneously.

Based on previous reports, oleic acid (OA) and oleylamine (OAm) are most widely used capping ligands in the preparation process of perovskites (named $CsPbX_3$ NCs-O).[13,16,31] OA can not only help to dissolve the precursors but also can suppressing the aggregation of NCs which contributes to the colloidal stability.[32,33] According to literature,[34] the $CsPbX_3$ perovskite NCs belong to ionic crystals, which are different from traditional NCs with stronger covalent properties. Thus, the intrinsic solubility equilibrium and dynamic ligand binding processes of $CsPbX_3$ perovskite NCs lead to serious degradation under high humidity and polar solvents.[35] Hence, organic molecules (OA and OAm) on the surface of perovskite NCs can be easily detached by ethyl acetate or *n*-hexane during purification due to high surface ligand dynamics mentioned above,[21,36] which may decrease the stability of perovskite NCs and promote its decomposition. As a result, the PLQYs of $CsPbX_3$ will be decreased with the leaving of ligands after purification.[34] Therefore, the binding ability of ligands is the key factor determining the stability of perovskite NCs.

On the basis of the above mentioned premises, we suppose that it is an alternative choice to keep the high PLQYs of $CsPbX_3$ perovskite NCs by enhancing the interaction between nanoparticles and ligands to ensure the sufficient binding ligands on their surface. According to literature, the melting point of ligands

[a]State Key Laboratory of Fine Chemicals, Dalian University of Technology, Dalian, P. R. China. E-mail: wusuli@dlut.edu.cn

[b]Qingdao University of Science and Technology, China

† Electronic supplementary information (ESI) available. See DOI: 10.1039/c8ra08102f

is a reasonable reference pointing to the ligand dynamics.[37] That is to say, the higher the melting point is, the lower ligand dynamic the ligand has. Therefore, it can be expected that if the commonly used OA (melting point = 13.4 °C) is replaced by ligands with high melting point, the mobility and the tendency of the ligand to leave the $CsPbX_3$ perovskite surface will decrease.[38] In other word, the binding ability of ligands mentioned above may higher than OA and the surface ligand coverage of ligands is expected to greatly increase and protect perovskite NCs more efficiently, which will keep the high PLQYs after purification. Meanwhile, the stability of $CsPbX_3$ NCs against water treatment, heating and photoradiation will be improved as well due to the coverage of ligands.

Here, tetradecanoic acid (TA, melting point is 52 °C), palmitic acid (PA, melting point is 63 °C), stearic acid (SA, melting point is 69.5 °C) and arachidic acid (AA, melting point is 74 °C) with only one anchoring group and a long hydrocarbon chain were selected to replace OA as ligands to prepare perovskite NCs. During purification and redispersion process, compared to OA and OAm, more ligands will stay on the crystal surface due to higher binding ability with $CsPbX_3$ NCs.[39] As a result, the $CsPbX_3$ perovskite NCs can be protected by them directly. Thus, the PLQYs of $CsPbX_3$ perovskite NCs can be maintained effectively. Furthermore, the long carbon chain structure has hydrophobic characteristics after interaction between carboxyl group and metal ions.[39,40] Thus, the stability of prepared $CsPbX_3$ perovskite NCs can be enhanced greatly. It is also worth to note that, the absolute photoluminescence quantum yield (PLQY) of the prepared $CsPbX_3$ perovskite NCs *via* PA and OAm as ligands reached 47–92%. Importantly, the PLQYs of $CsPbX_3$ perovskite NCs can be sustained for one month with a small decrease. The obtained $CsPbBr_3$ NCs can be dispersed in organic solvents to form stable luminescent ink. Meanwhile, we also fabricate a WLEDs by combining an InGaN LED (460 nm) with $CsPbBr_3$ and $CsPbI_3$ NCs as green and red phosphors directly.

Experimental section

Chemicals

Cs_2CO_3, trioctylphosphine oxide, $PbCl_2$, $PbBr_2$, PbI_2, OAm, OA were obtained from Aladdin. Tetradecanoic acid, palmitic acid and stearic acid were purchased from Tianjin Bodi Chemical Co. Ltd. Arachidic acid was obtained from Ark Pharm. The chemicals were used as received without any further purification.

Preparation of Cs-stearate

Cs_2CO_3 (0.16 g) was loaded into 50 mL 3-neck flask along with octadecene (6 mL) and stearic acid (1.1 g), heated for 1 h at 120 °C, and then heated under N_2 to 150 °C until all Cs_2CO_3 was dissolved. Since Cs-stearate precipitates out of ODE at room-temperature, it has to be preheated to 120 °C before injection.

Synthesis of $CsPbBr_3$ NCs

The synthesis of $CsPbBr_3$ refers to the previous method with some revisions.[13] In detail, ODE (octadecene, 5 mL) in 50 mL four-neck flask was heated to 120 °C. SA (stearic acid, 1.06 g) and OAm (OAm, 1 mL) were injected into the ODE under N_2 flow, and then 0.4 mL Cs-stearate was quickly injected. Finally, the mixture was heated to 160 °C for 5 s and cooled quickly by ice-water bath. The as-grown product was centrifuged at speed of 9000 rpm for 5 min and the precipitates were dispersed in *n*-hexane, followed by centrifuging at 9000 rpm for 10 min. Finally, the precipitates were collected and then dispersed with 20 mL *n*-hexane.

The samples fabricated *via* OA/OAm, TA/OAm, PA/OAm, SA/OAm and AA/OAm were named as $CsPbX_3$ (X = Cl/Br, Br and I) NCs-O, $CsPbX_3$ (X = Cl/Br, Br and I) NCs-T, $CsPbX_3$ (X = Cl/Br, Br and I) NCs-P, $CsPbX_3$ (X = Cl/Br, Br and I) NCs-S and $CsPbX_3$ (X = Cl/Br, Br and I) NCs-A respectively.

Fabrication of WLED devices

The $CsPbBr_3$ and $CsPbI_3$ perovskite NCs were prepared using PA/OAm as ligand. Firstly, 0.05 g of silicone resin A and 0.1 g of silicone resin B were mixed with 0.015 g $CsPbBr_3$ perovskite NCs; secondly, 0.01 g of $CsPbI_3$ perovskite NCs were mixed with 0.05 g of silicone resin A and 0.2 g of silicone resin B; then the mixture mentioned above were mixed and stirred thoroughly. Afterward, the mixtures were deposited on a 460 nm InGaN LED chip.

Characterization

The morphologies of the samples were determined by using a Nova Nanosem 450 field emission scanning electron microscopy (FE-SEM) and a Tecnai F20 S-TWIN micro-scope transmission electron microscope operating at 200 kV (TEM). Powder X-ray diffraction patterns were measured on a Rigaku D/MAX-2400 diffractometer with Cu-Kα radiation. FT-IR spectra of the samples were characterized using the FT-IR method (NICOLET 6700, Thermo SCIENTIFIC). The XPS patterns were acquired by X-ray Photoelectron Spectrometer (ESCALAB™ 250Xi, Thermo Fisher). UV-Vis spectra were obtained from aqueous suspensions using an UV-Vis spectrophotometer (JASCO UV-550). Fluorescence decay traces of perovskite NCs were recorded in the Time Correlated Single Photon Counting (TCSPC) mode using the FLS920 Spectrofluorometer (Edinburgh Instruments, UK). The PL spectra of the perovskite NCs were obtained by using F-7000 Fluorescence Spectrophotometer (Hitachi, Japan). The optical properties of WLEDs were obtained using Keithley 2400 and KONICA MINOLTA CS200. The quantum yield (PLQYs) measurements were recorded using an integrating sphere, recorded on an Edinburgh Instruments FLS920 spectrophotometer. ^{1}H NMR measurements were recorded on a Bruker Avance III 500 MHz spectrometer.

Result and discussion

Based on previous reports, on increasing the melting pointing of ligands, the mobility of the ligand to leave the crystal surface will decrease due to the enhanced binding ability.[37,38] Thus, much more ligands with high binding ability will stay on the surface of perovskite NCs. In other word, compared to the usually used OA (melting point is 13.4 °C), the tendency of SA (melting point is 69.5 °C) to leave the crystal surface will

decrease.[39] As known to all, the PLQYs and stability are significant influenced by surface ligands.[41] Hence, aimed to alleviated the effect of ligands on the luminescent properties, SA was first selected in this work to replace OA as ligand to prepare perovskite NCs (denoted as NCs-S), because it has the same carbon chain length and functional group with OA, but higher binding ability than OA. As a control experiment, OA was also used as ligand to synthesize perovskite NCs (denoted as NCs-O). As depicted in Scheme 1, due to the lower tendency of SA to leave the surface of perovskite NCs, after purification and redispersion process by hexane, the coverage of SA on surface of NCs should be much higher than that of OA (Scheme 1).

$CsPbX_3$ NCs were synthesized according to previously reported method, except SA was used to couple with OAm as ligands.[13] To investigate the effect of SA on the properties of obtained $CsPbX_3$ perovskite NCs, the morphology and crystal phase were characterised by transmission electron microscopy (TEM) and high resolution TEM (HR-TEM) (Fig. 1A and B). As shown in Fig. 1A, the TEM image of $CsPbBr_3$ perovskite NCs indicates the presence of irregular surrounding around perovskite NCs, which is similar with that embedded within the organic matter or polymer.[20,42] Meanwhile, the obtained particles were separated from each other, preventing the agglomeration effectively. In other word, the long distance between NCs caused by the existence of SA inhibits the close contact and regrowth possibility, which is beneficial to keep the high PLQY and improve the stability of $CsPbBr_3$ perovskite NCs.[7] Furthermore, HR-TEM image in Fig. 1B shows that the lattice space of the prepared $CsPbBr_3$ perovskite NCs is 0.29 nm, which is in good agreement with the (200) plane of cubic perovskite $CsPbBr_3$ phase. These results prove the formation of cubic $CsPbBr_3$ perovskite NCs. In addition, the elemental mapping also prove the uniform distribution of elements in the prepared $CsPbBr_3$ NCs (Fig. S1†). In sharp contrast, the $CsPbBr_3$ NCs synthesized by OA as ligand are cubic particles with a tendency to self-assembled into agglomerates on the TEM grids (Fig. 1C and D), as previously reported.[26] Thus, the larger particles will tend be formed and the emission spectrum will become broad.[7] The difference confirmed that using SA as ligand can inhibit the agglomerate of NCs and thereby avoid their regrowth induced instability.

For the application of $CsPbX_3$ perovskite NCs, an important issue is their PLQYs. In this regard, the PLQYs of $CsPbX_3$ NCs obtained *via* SA and OAm purified *via* *n*-hexane were measured. Unfortunately, the PLQYs of the obtained $CsPb(Cl_{0.6}Br_{0.4})_3$, $CsPbBr_3$ and $CsPbI_3$ NCs *via* SA are only 15%, 46% and 26%, which are lower than that synthesized by OA and OAm in previous reports.[13] The low PLQYs may be ascribed to the surface defects caused by the variation of ligands during the synthesis of $CsPbX_3$ NCs.[11,15] The HR-TEM images in Fig. 1B and

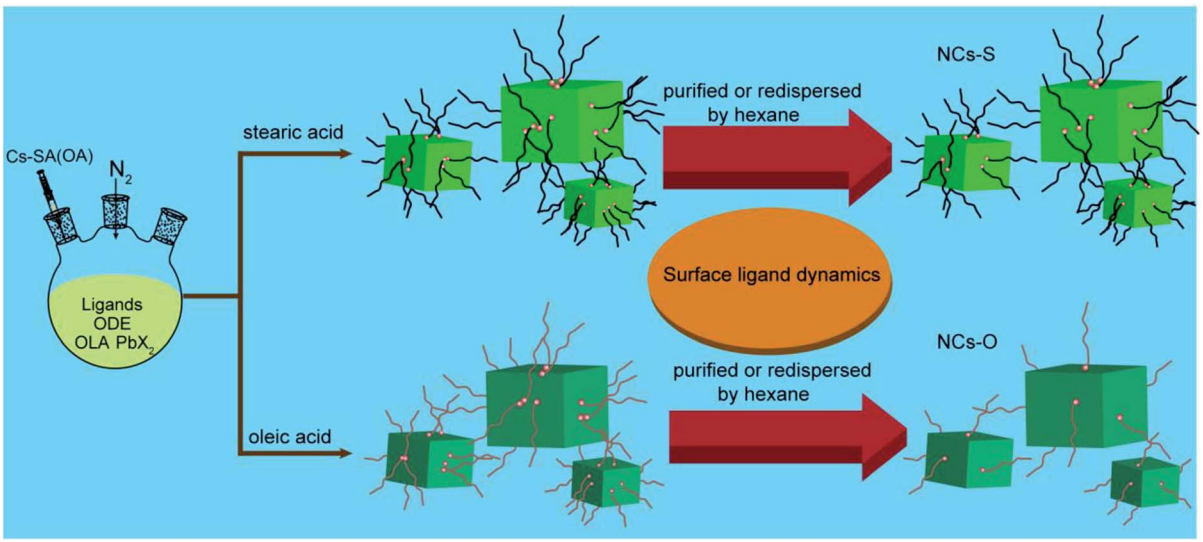

Scheme 1 Schematic of ligands leaving the crystal surface.

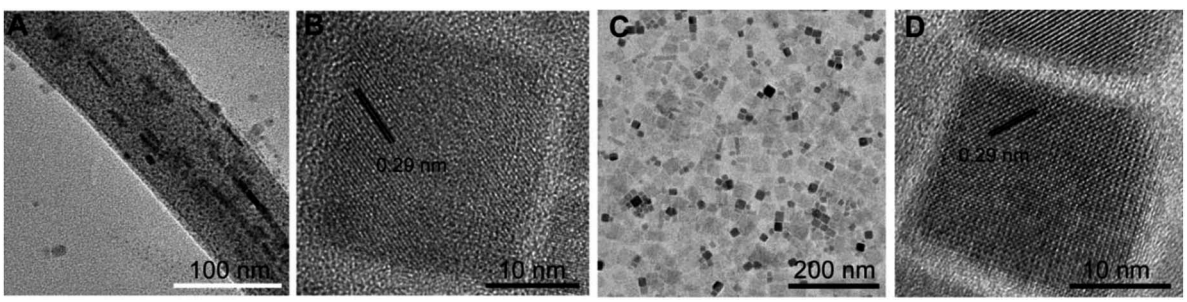

Fig. 1 (A and B) TEM and HRTEM images of $CsPbBr_3$ fabricated *via* SA; (C and D) TEM and HRTEM images of $CsPbBr_3$ fabricated *via* OA.

D prove that the crystallinity of $CsPbX_3$ NCs obtained *via* SA and OAm is not as perfect as that of NCs prepared using OA and OAm as ligands, which will decrease their PLQYs.[7,25]

Thus, aimed to obtain $CsPbX_3$ NCs with higher PLQYs and better stability after purification. We further selected TA, PA and AA to couple with OAm as ligands to prepare perovskite NCs, which are denoted as NCs-T, NCs-P and NCs-A, respectively. TEM images illustrate that the prepared $CsPbBr_3$ NCs-T (Fig. 2A), $CsPbBr_3$ NCs-P (Fig. 2B) and $CsPbBr_3$ NCs-A (Fig. 2C) are also surrounded by amorphous matters similar as embedded in the organic matter or polymer, which will provide them with good stability.[20,42] In addition, the high-resolution TEM (insets) images in Fig. 2A–C show that the lattice spaces of the prepared $CsPbBr_3$ perovskite NCs are 0.29 nm, which are in good agreement with the (200) plane of cubic perovskite $CsPbBr_3$ synthesized *via* OA (Fig. 1D) and SA (Fig. 1B). Furthermore, the XPS spectra of the $CsPbBr_3$ NCs-P are shown in Fig. S2.† Peaks originating from Cs 3d, Pb 4f and Br 3d electrons are observed, and the energies are consistent with $CsPbBr_3$ perovskite NCs.[34] All these results confirm that the $CsPbBr_3$ NCs with cubic shape can also be obtained *via* TA, PA and AA as ligands. It is worth to note that the morphology and crystallinity of $CsPbBr_3$ NCs-P are more perfect than the other two NCs.

We next measured the PL spectra of obtained $CsPbBr_3$ NCs obtained using different ligands at the same concentration. As shown in Fig. S3,† the PL intensity of $CsPbBr_3$ NCs-P is obviously higher than others. This difference may be ascribed to the

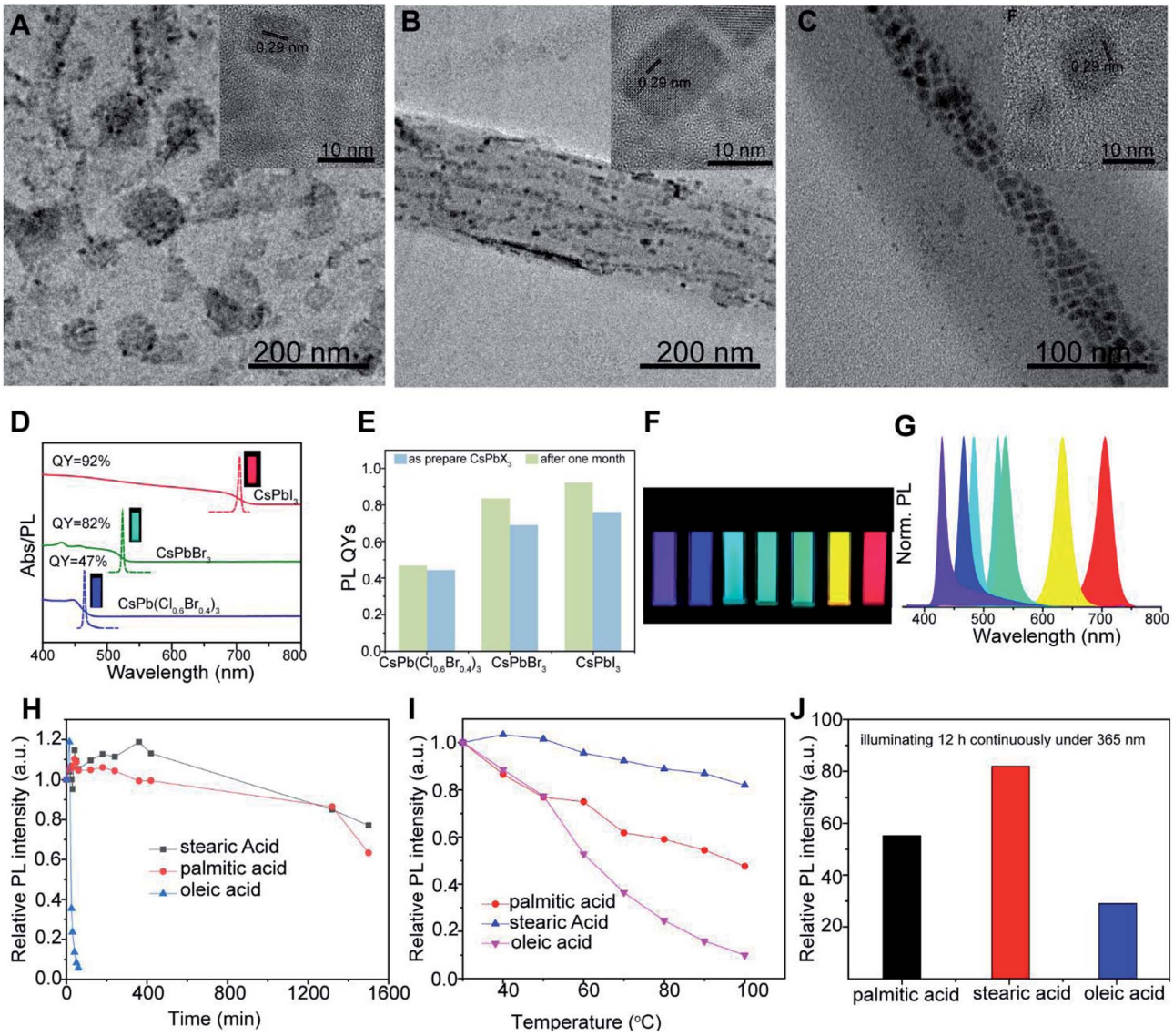

Fig. 2 TEM and HR-TEM images (insets) of $CsPbBr_3$ fabricated *via* TA (A), PA (B) and AA (C); (D) typical optical absorption, PL spectra and PL QYs of $CsPb(Br_{0.4}Cl_{0.6})_3$, $CsPbBr_3$ and $CsPbI_3$; (E) the PLQYs of $CsPb(Cl_{0.6}Br_{0.4})_3$, $CsPbBr_3$ and $CsPbI_3$ obtained *via* PA and OAm before and after stored at room temperature a month; (F) the photographs of $CsPb(Br_{0.3}Cl_{0.7})_3$, $CsPb(Br_{0.4}Cl_{0.6})_3$, $CsPbBr_3$, $CsPb(I_{0.4}Br_{0.6})_3$, $CsPb(I_{0.5}Br_{0.5})_3$, $CsPb(I_{0.7}Br_{0.3})_3$ and $CsPbI_3$ solutions (from left to right) in hexane under UV lamp ($\lambda = 365$ nm); (G) the representative PL spectra ($\lambda_{exc} = 365$ nm) for the samples corresponding to Fig. 2F; (H) water resistance test of the $CsPbBr_3$ NCs-O, $CsPbBr_3$ NCs-P and $CsPbBr_3$ NCs-S; (I) thermal stability test of the $CsPbBr_3$ NCs-O, $CsPbBr_3$ NCs-P and $CsPbBr_3$ NCs-S; (J) photostability test of the $CsPbBr_3$ NCs-O, $CsPbBr_3$ NCs-P and $CsPbBr_3$ NCs-S.

reason that the changing of ligands during the synthesis of $CsPbBr_3$ NCs may lead to different surface property and crystallinity of $CsPbBr_3$ NCs, which are closely related to their PLQYs.[11,15]

Further, the $CsPb(Cl_{0.6}Br_{0.4})_3$, $CsPbBr_3$ and $CsPbI_3$ with blue, green and red colors were synthesized *via* PA and OAm as ligands and their PLQYs were measured (as shown in Fig. 2D). Excitingly, the PLQYs of the obtained $CsPb(Cl_{0.6}Br_{0.4})_3$, $CsPbBr_3$ and $CsPbI_3$ reached 47%, 82% and 92%, respectively. Furthermore, as shown in Fig. 2E, all the $CsPb(Cl_{0.6}Br_{0.4})_3$, $CsPbBr_3$ and $CsPbI_3$ retain their high QY in solution and only slightly decrease after one month of storage at room temperature (~28 °C, relative humidity of ~80%). Hence, we take PA and OAm as ligands to synthesize perovskite NCs with different colors and investigate their PL properties and applications. As shown in Fig. 2F, the color of the solution can be steadily tuned from violet to blue, green, orange and red. The emission peaks of such $CsPbX_3$ perovskite NCs can be readily tuned between 429 nm ($CsPb(Cl_{0.7}Br_{0.3})_3$) and 705 nm ($CsPbI_3$), covering the entire visible-light range (Fig. 2G). The full-width at half maximum (fwhm) of emission spectra are only 15–30 nm, confirming the high uniformity of prepared NCs.

Importantly, the stability of these NCs fabricated *via* PA and SA against water, heating and photo radiation were greatly enhanced as well (as shown in Fig. 2H–J). Besides that, the PL emission peak location of $CsPbBr_3$ NCs-P kept almost unchanged during against water, heating and photo radiation, while the emission peaks of NCs-O were red shifted (Fig. S4†) may be caused by the size increase of $CsPbBr_3$ NCs-O.[6] Additionally, the water resistance tests for $CsPbBr_3$ NCs prepared using other ligands were also performed (Fig. S5†). It is worth noting that the water resistance stability decrease in this order: $CsPbBr_3$ NCs-S > $CsPbBr_3$ NCs-P > $CsPbBr_3$ NCs-T > $CsPbBr_3$ NCs-O, which is consistent with the order of binding ability: SA > PA > TA > OA. During the preparation of different $CsPbBr_3$ NCs, the experimental conditions and chemicals are the same except the different ligands. Thus, it is rational to ascribe this stability variation to the difference in ligands. The increase in the binding ability of the ligands is strongly dependent on the interligand interaction.[37] Therefore, as the tendency of leaving the crystal surfaces of the ligands decreases with the increase binding ability of the ligands, so does the surface ligand dynamic population.[38] As a result, the $CsPbBr_3$ NCs obtained *via* high binding ability is more stable. All these results indicate that using ligands with high binding ability to replace commonly used OA, perovskite NCs with both high QY and good stability can be achieved.

Considering the fact that $CsPbX_3$ is belong to ionic crystal, the interaction with capping ligand is ionic[43] and the solubility equilibrium in solvent is not only related to perovskite's intrinsic crystal feature, but also influenced by the types of ligands.[36] Hence, the PLQYs of $CsPbX_3$ NCs are affected by the types and the covering degree of ligands. To further confirm the good stability and high PLQYs of $CsPbX_3$ NCs prepared using PA as ligands are ascribed to the high binding ability of PA, the ^1H solution nuclear magnetic resonance spectroscopy (NMR) was used to analyze the amount of surface ligands and thereby prove their binding ability with $CsPbBr_3$ NCs.[34] Before that, the FTIR spectra of PA and the product are shown in Fig. S6† to prove the existence of ligands.[3] Furthermore, as shown in Fig. S7,† the concentration of organic components determined from resonance 1 (ascribe to α-H) in the solution of $CsPbBr_3$ NCs-O purified twice by *n*-hexane is far less than the organic components composed of PA and OAm in the solution of $CsPbBr_3$ NCs-P. Hence, this result proves that more ligands can be bound with $CsPbBr_3$ NCs-P compared to $CsPbBr_3$ NCs-O after purification.

Additionally, the ^1H NMR was also used to characterize the different binding ability by analysing the mixture of different ligands and purified $CsPbBr_3$ solution. Before ^1H NMR measurement, $CsPbBr_3$ NCs were purified by *n*-hexane and ethyl acetate to remove the non-binding free ligand.[34] Then, the same amount of PA or OA as well as OAm were added into the chloroform-d solution of purified $CsPbBr_3$ NCs (the experimental process is provided in the ESI† in detail and the ^1H NMR of purified $CsPbBr_3$ NCs is shown in Fig. S8†). The total concentration of the organic species bound to NCs can be expressed by NMR spectra. As shown in Fig. S9,† comparing with the spectra of OA, OAm and PA, we recognize the characteristic resonances 1 and 2 of OA and PA in the samples. Unfortunately, the overlap between resonance 2 and resonance 3 would influence the judgement of the variation of acids before and after the addition of $CsPbBr_3$ NCs. Thus, we select resonance 1 to describe the change of concentration of the alkyl acids. As shown in Fig. 3, after addition of $CsPbBr_3$ NCs, the decrease of resonance 1 in PA and OAm system is obviously greater than that in OA and OAm system, which means much more ligands are bound with $CsPbBr_3$ NCs when OA is replaced by PA as ligands. This result can further explain the reason why the $CsPbBr_3$ NCs-P displays higher PLQY and stability than $CsPbBr_3$ NCs-O. Furthermore, the effects of different ligands (PA and OA) on the PL intensities and PLQYs of purified $CsPbBr_3$ NCs were also performed (the experimental process is provided in the ESI† in detail). As shown in Fig. 3C, the PL intensities and PLQYs increase in this order: $CsPbBr_3$ NCs < $CsPbBr_3$ NCs with OA (OAm) < $CsPbBr_3$ NCs with PA (OAm). As mentioned above, the PLQYs increase in this order: $CsPbBr_3$-O < $CsPbBr_3$-S < $CsPbBr_3$-P. In addition, the lifetimes of the $CsPbBr_3$-O, $CsPbBr_3$-P and $CsPbBr_3$-S are 21 ns, 11 ns and 14 ns respectively (Fig. S10†). The perovskite nanocrystal with the different capping ligands have a clear correlation with the PLQYs, which is consistent with the previous report.[44] Based on above results, the ligands composed of PA and OAm are more beneficial to the PL intensities and PLQYs of $CsPbX_3$ NCs.

In previous report,[45] when OA and OAm were replaced by high binding ability ligands SA and octadecylamine (ODA), the $FAPbX_3$ NCs with high PLQY and enhanced stability have been synthesized successfully. The application of high binding ability ligand alkylamine may also influence the PLQY of $CsPbBr_3$ NCs. Thus, as a control experiment, the $CsPbBr_3$ NCs are also fabricated *via* PA and hexadecylamine (HA) as ligands rather than PA and OAm. Compared with $CsPbBr_3$ NCs-P, the PL intensity and quantum yield (24%) are relatively low (as shown in Fig. S11†). Therefore, we can conclude that the application of OAm is also important for the high PLQY of $CsPbX_3$ NCs.

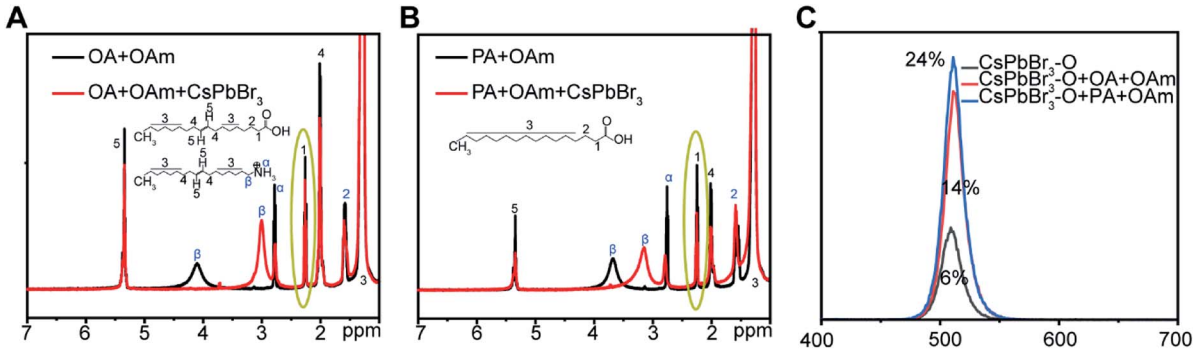

Fig. 3 (A) The ^{1}H NMR spectra of chloroform-d solution containing OA and OAm before and after the addition of purified $CsPbBr_3$ NCs-O; (B) ^{1}H NMR spectra of PA and OAm before and after the addition of purified $CsPbBr_3$ NCs-P; (C) the PL intensities and PLQYs of pure $CsPbBr_3$ NCs-O, $CsPbBr_3$ NCs-O + OA + OAm and $CsPbBr_3$ NCs-O + PA + OAm.

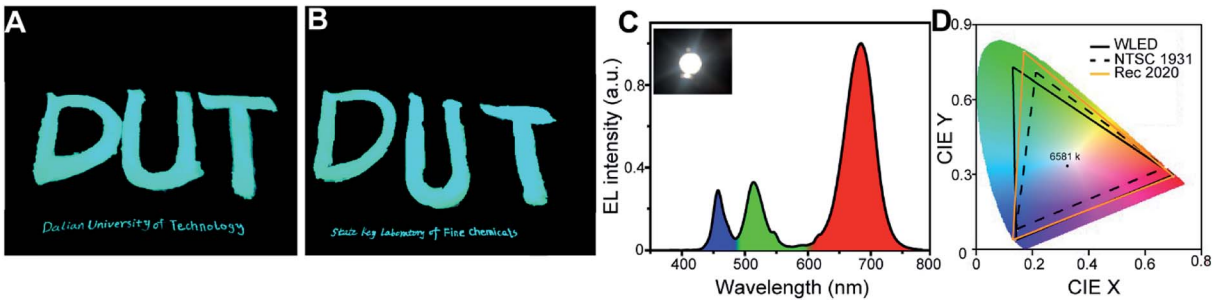

Fig. 4 Photographs of handwritten "DUT", "Dalian University of Technology" and "State Key Laboratory of Fine Chemicals" patterns on the filter papers *via* writing brush and pen using $CsPbBr_3$ NCs-S (A) and $CsPbBr_3$ NCs-P (B) irradiated by UV light; (C) emission spectrum of WLED fabricated by mixing green $CsPbBr_3$ NCs and red $CsPbI_3$ NCs deposited on a blue-emitting InGaN LED chip; (D) the color gamut of the WLED (solid line), compared to the NTSC (dashed line) and the Rec.2020 (yellow line) standards.

The $CsPbBr_3$ NCs obtained using PA and SA (Fig. 2H–J) as ligands can be well-dispersed in *n*-hexane with good colloidal stability, which enable them can be used as a solution luminescent ink. As shown in Fig. 4(A and B), "DUT" patterns were handwritten on a piece of filter paper using a writing brush. Furthermore, "Dalian University of Technology" and "State Key Laboratory of Fine Chemicals" were also handwritten on the filter papers by a common pen. The patterns exhibit strong PL emission under UV light. Thanks to the sufficient ligands on the surface of NCs owing to the high binding ability, the bright PL emission is preserved even after 7 days without any protection under a relative humidity (RH) of 40–60% (Fig. S12†).

Especially, such a high PLQY, versatile tunable colors, narrow emission bands and the remarkable stability also make the $CsPbX_3$ NCs an outstanding candidate as a phosphor material for lighting and backlight display application. In the previous works, most of the WLEDs were fabricated through combining green-emitting perovskite NCs with a red emitting K_2SiF_6:Mn^{4+} or CdSe as phosphor.[8,20,25,33] In this method, we mixed the green $CsPbBr_3$ NCs-P and red $CsPbI_3$ NCs-P directly as phosphors without the use of any other commercial phosphors. Thus, the WLED can be fabricated by embedding $CsPbI_3$ (red) and $CsPbBr_3$ (green) as phosphors into silicone resin and coating them on a blue InGaN LED chip emitting at 460 nm with diameter of 3 mm. Fig. 4E shows the luminescence spectrum of the fabricated WLED device operating at 10 mA, composing three emission peaks: green and red ones originating from the perovskite NCs, and the blue one deriving from the LED chip. The photograph of the operating WLED is also shown as an inset in Fig. 4C. The CIE *xy* coordinates of the WLED output are (0.31, 0.34) corresponding to a white correlated color temperature of 6581 K. At a diode current of 10 mA, the luminous efficacy of the WLED is 2.1 lm W^{-1}, which is similar with that reported by Ye.[28] The values that could potentially be increased by optimizing the packaging process and composites. Furthermore, the color gamut of the WLED is presented in Fig. 4D (solid line), covering 125% of the NTSC gamut (dashed line) 86% of the Rec.2020 gamut (yellow line), which was higher than that of previously phosphor LED.[8,20,22,28] The enhanced color gamut can be attributed to the narrow emission wavelength of $CsPbX_3$ perovskite NCs.[23]

Conclusion

In summary, $CsPbX_3$ perovskite NCs with high quantum yield and chemical stability are synthesized utilizing PA and OAm as ligands. ^{1}H NMR characterizations confirm that the more ligands will be bound with $CsPbX_3$-P than $CsPbX_3$-O. The emission color of perovskites NCs obtained using PA as ligand can be tuned in the whole visible region with high luminesce intensity and narrow full width at half-maximum. Particularly, the $CsPbX_3$ (X = Cl/Br, Br and I) NCs with high yield (47–92%)

can be prepared. More importantly, the high QYs can be sustained for at least one month due to the stronger binding ability of PA and OAm. These perovskite NCs can be used as stable luminescent inks and phosphors for white light-emitting diodes with a wide color gamut. This work may open a new way to realize perovskites NCs with high stability and high quantum yield simultaneously, and promote their application in luminescent ink and LED.

Conflicts of interest

There are no conflicts to declare.

Acknowledgements

This work was supported by the National Natural Science Foundation of China (21476040, 21276040, 21536002) and the Program for Changjiang Scholars and Innovative Research Team in the University (IRT0711), Fund for innovative research groups of the National Natural Science Fund Committee of Science (21421005) and the Fundamental Research Funds for the Central Universities (DUT16TD25, DUT2016TB12).

References

1 A. B. Wong, M. Lai, S. W. Eaton, Y. Yu, E. Lin, L. Dou, A. Fu and P. Yang, *Nano Lett.*, 2015, **15**, 5519.
2 J. H. Im, I.-H. Jang, N. Pellet, M. Grätzel and N. G. Park, *Nat. Nanotechnol.*, 2014, **9**, 927.
3 W. Zhang, M. Anaya, G. Lozano, M. E. Calvo, M. B. Johnston, H. Míguez and H. J. Snaith, *Nano Lett.*, 2015, **15**, 1698.
4 W. S. Yang, B.-W. Park, E. H. Jung, N. J. Jeon, Y. C. Kim, D. U. Lee, S. S. Shin, J. Seo, E. K. Kim, J. H. Noh and S. I. Seok, *Science*, 2017, **356**, 1376.
5 P. Ramasamy, D.-H. Lim, B. Kim, S. H. Lee, M. S. Lee and J. S. Lee, *Chem. Commun.*, 2016, **52**, 2067.
6 I. Levchuk, A. Osvet, X. Tang, M. Brandl, J. D. Perea, F. Hoegl, G. J. Matt, R. Hock, M. Batentschuk and C. J. Brabec, *Nano Lett.*, 2017, **17**, 2765.
7 X. Li, Y. Wang, H. Sun and H. Zeng, *Adv. Mater.*, 2017, **29**, 1701185.
8 M. Chen, Y. Zou, L. Wu, Q. Pan, D. Yang, H. Hu, Y. Tan, Q. Zhong, Y. Xu, H. Liu, B. Sun and Q. Zhang, *Adv. Funct. Mater.*, 2017, **27**, 1701121.
9 J. Xu, W. Huang, P. Li, D. R. Onken, C. Dun, Y. Guo, K. B. Ucer, C. Lu, H. Wang, S. M. Geyer, R. T. Williams and D. L. Carroll, *Adv. Mater.*, 2017, **29**, 1703703.
10 D. N. Dirin, I. Cherniukh, S. Yakunin, Y. Shynkarenko and M. V. Kovalenko, *Chem. Mater.*, 2016, **28**, 8470.
11 A. Pan, B. He, X. Fan, Z. Liu, J. J. Urban, A. P. Alivisatos, L. He and Y. Liu, *ACS Nano*, 2016, **10**, 7943.
12 J. Song, L. Xu, J. Li, J. Xue, Y. Dong, X. Li and H. Zeng, *Adv. Mater.*, 2016, **28**, 4861.
13 L. Protesescu, S. Yakunin, M. I. Bodnarchuk, F. Krieg, R. Caputo, C. H. Hendon, R. X. Yang, A. Walsh and M. V. Kovalenko, *Nano Lett.*, 2015, **15**, 3692.
14 Z. Long, H. Ren, J. Sun, J. Ouyang and N. Na, *Chem. Commun.*, 2017, **53**, 9914.
15 S. Wei, Y. Yang, X. Kang, L. Wang, L. Huang and D. Pan, *Chem. Commun.*, 2016, **52**, 7265.
16 Y. Tong, E. Bladt, M. F. Aygüler, A. Manzi, K. Z. Milowska, V. A. Hintermayr, P. Docampo, S. Bals, A. S. Urban, L. Polavarapu and J. Feldmann, *Angew. Chem., Int. Ed.*, 2016, **55**, 13887.
17 X. Hu, H. Zhou, Z. Jiang, X. Wang, S. Yuan, J. Lan, Y. Fu, X. Zhang, W. Zheng, X. Wang, X. Zhu, L. Liao, G. Xu, S. Jin and A. Pan, *ACS Nano*, 2017, **11**, 9869.
18 D. Zhang, S. W. Eaton, Y. Yu, L. Dou and P. Yang, *J. Am. Chem. Soc.*, 2015, **137**, 9230.
19 X. Tang, Z. Zu, H. Shao, W. Hu, M. Zhou, M. Deng, W. Chen, Z. Zang, T. Zhu and J. Xue, *Nanoscale*, 2016, **8**, 15158.
20 T. Xuan, X. Yang, S. Lou, J. Huang, Y. Liu, J. Yu, H. Li, K.-L. Wong, C. Wang and J. Wang, *Nanoscale*, 2017, **9**, 15286.
21 Q. Shan, J. Song, Y. Zou, J. Li, L. Xu, J. Xue, Y. Dong, B. Han, J. Chen and H. Zeng, *Small*, 2017, **13**, 1701770.
22 H. C. Wang, S. Y. Lin, A. C. Tang, B. P. Singh, H. C. Tong, C. Y. Chen, Y. C. Lee, T. L. Tsai and R.-S. Liu, *Angew. Chem., Int. Ed.*, 2016, **55**, 7924.
23 J. Hai, H. Li, Y. Zhao, F. Chen, Y. Peng and B. Wang, *Chem. Commun.*, 2017, **53**, 5400.
24 S. N. Raja, Y. Bekenstein, M. A. Koc, S. Fischer, D. Zhang, L. Lin, R. O. Ritchie, P. Yang and A. P. Alivisatos, *ACS Appl. Mater. Interfaces*, 2016, **8**, 35523.
25 S. Lou, T. Xuan, C. Yu, M. Cao, C. Xia, J. Wang and H. Li, *J. Mater. Chem. C*, 2017, **5**, 7431.
26 H. Huang, B. Chen, Z. Wang, T. F. Hung, A. S. Susha, H. Zhong and A. L. Rogach, *Chem. Sci.*, 2016, **7**, 5699.
27 L. Gomez, C. de Weerd, J. L. Hueso and T. Gregorkiewicz, *Nanoscale*, 2017, **9**, 631.
28 J.-Y. Sun, F. T. Rabouw, X.-F. Yang, X.-Y. Huang, X.-P. Jing, S. Ye and Q.-Y. Zhang, *Adv. Funct. Mater.*, 2017, **27**, 1704371.
29 Y. Wei, X. Deng, Z. Xie, X. Cai, S. Liang, P. a. Ma, Z. Hou, Z. Cheng and J. Lin, *Adv. Funct. Mater.*, 2017, **27**, 1703535.
30 Z. J. Li, E. Hofman, J. Li, A. H. Davis, C. H. Tung, L. Z. Wu and W. Zheng, *Adv. Funct. Mater.*, 2018, **28**, 1704288.
31 X. Zhang, H. Lin, H. Huang, C. Reckmeier, Y. Zhang, W. C. H. Choy and A. L. Rogach, *Nano Lett.*, 2016, **16**, 1415.
32 L. Wu, Q. Zhong, D. Yang, M. Chen, H. Hu, Q. Pan, H. Liu, M. Cao, Y. Xu, B. Sun and Q. Zhang, *Langmuir*, 2017, **33**, 12689.
33 F. Zhang, H. Zhong, C. Chen, X.-g. Wu, X. Hu, H. Huang, J. Han, B. Zou and Y. Dong, *ACS Nano*, 2015, **9**, 4533.
34 J. H. Li, L. M. Xu, T. Wang, J. Z. Song, J. W. Chen, J. Xue, Y. H. Dong, B. Cai, Q. S. Shan, B. N. Han and H. B. Zeng, *Adv. Mater.*, 2017, **29**, 1603885.
35 S. Hou, Y. Z. Guo, Y. G. Tang and Q. M. Quan, *ACS Appl. Mater. Interfaces*, 2017, **9**, 18417.
36 X. Li, D. Yu, F. Cao, Y. Gu, Y. Wei, Y. Wu, J. Song and H. Zeng, *Adv. Funct. Mater.*, 2016, **26**, 5903.
37 N. Pradhan, D. Reifsnyder, R. Xie, J. Aldana and X. Peng, *J. Am. Chem. Soc.*, 2007, **129**, 9500.
38 S. Wu, Y. Liu, J. Chang and S. Zhang, *CrystEngComm*, 2014, **16**, 4472.

39 B. B. Srivastava, S. Jana, D. D. Sarma and N. Pradhan, *J. Phys. Chem. Lett.*, 2010, **1**, 1932.
40 N. Bogdan, F. Vetrone, G. A. Ozin and J. A. Capobianco, *Nano Lett.*, 2011, **11**, 835.
41 L. Qu and X. Peng, *J. Am. Chem. Soc.*, 2002, **124**, 2049.
42 A. Pan, M. J. Jurow, F. Qiu, J. Yang, B. Ren, J. J. Urban, L. He and Y. Liu, *Nano Lett.*, 2017, **17**, 6759.
43 J. D. Roo, M. Ibáñez, P. Geiregat, G. Nedelcu, W. Walravens, J. Maes, J. C. Martins, I. V. Driessche, M. V. Kovalenko and Z. Hens, *ACS Nano*, 2016, **10**, 2071.
44 J. R. Lakowicz, C. D. Geddes, I. Gryczynski, J. Malicka, Z. Gryczynski, K. Aslan, J. Lukomska, E. Matveeva, J. Zhang, R. Badugu and J. Huang, *J. Fluoresc.*, 2004, **14**, 425.
45 Q. H. Li, H. Y. Li, H. B. Shen, F. F. Wang, F. Zhao, F. Li, X. G. Zhang, D. Y. Li, X. Jin and W. F. Sun, *ACS Photonics*, 2017, **4**, 2504.